

## Abstract

Angle-dependent magnetoresistance oscillations have been used to identify two distinct inelastic scattering channels in the high temperature copper-oxide superconductor  $Tl_2Ba_2Ca_0Cu_1O_{6+\delta}$  (Tl2201). One of these channels is found to be isotropic around the Fermi Surface with a magnitude proportional to  $T^2$ . The other channel is found to be highly anisotropic with the same four fold symmetry as the superconducting gap and a magnitude that grows linearly with temperature. Significantly, this form of scattering rate can account for the temperature dependence of both the in-plane resistivity and Hall effect at this particular doping level. At fixed temperature we identify an approximately linear correlation between a normal state property (the magnitude of the anisotropic scattering) and  $T_c$  which, intriguingly extrapolates to zero at the doping level where superconductivity vanishes.

## Introduction

A key step in gaining an understanding of high temperature superconductors is generally regarded as understanding the properties of their normal state which occurs when the superconductivity is suppressed in some way. The  $T_c$  of Cu-O based superconductors can be changed by doping the crystal structure, usually by the removal or addition of oxygen (e.g. Tl2201) or the substitution of ions (e.g. LSCO) – see Fig. 1. For overdoped samples the temperature dependence of the resistivity generally fits to  $A+BT+CT^2$  with the  $T^2$  term beginning to dominate as doping increases. The inverse Hall angle  $\cot\theta_H$  fits to  $A+CT^2$  [1]. There is clearly a difference in these temperature dependences suggesting that the mechanisms responsible might not be the same.

## $Tl_2Ba_2Ca_0Cu_1O_{6+\delta}$

Tl2201 is one of the cleanest copper-oxide based superconductors with a low residual resistivity and low upper critical field. Its  $T_c$  can be adjusted anywhere from optimally doped ( $T_c \approx 90K$ ) to overdoped by annealing in an oxygen or argon atmosphere. The band-structure in Fig. 1 shows a large hole pocket around the X point of the Brillouin zone and a small electron pocket around the  $\Gamma$  point (which is not seen by AMRO or ARPES [2] studies).

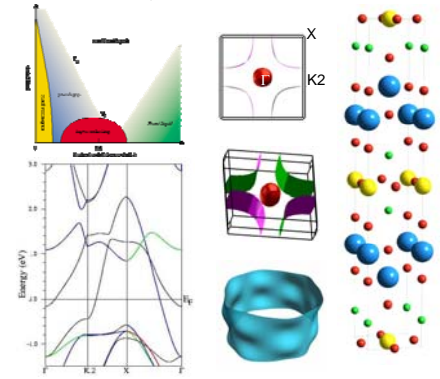


Fig. 1 – Top Left: generic HTSC phase diagram. Bottom Left: Undoped Tl2201 bandstructure (Wien2K). Right: Undoped Tl2201 crystal structure. Blue=Ti, Green=Ba, Yellow=Cu, Red=O. Center: Tl2201 Fermi surface - Top and Middle: Wien2K & Bottom: from AMRO fitting parameters.

## AMRO

Angle-dependent Magneto-Resistance Oscillations occur in the interlayer resistivity when a sample is rotated with respect to a magnetic field of fixed intensity at constant temperature.

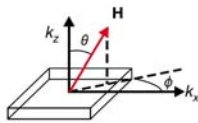


Fig. 2 – AMRO sample geometry.

In a large magnetic field electrons are driven around the Fermi surface in orbits in the plane perpendicular to the applied field. Maxima in the interlayer resistivity occur when the area of all the orbits is identical. Equivalently, this is when the interplane velocity averaged around the Fermi surface is zero. Clearly for a simple cylinder no effect would be seen. Contrastingly, for a barrel shaped Fermi surface Yamaji [3] showed that the field angles at resistivity maxima occur are given by  $\cot\theta_H = \pi(n-1/4)$ , see Fig. 3.

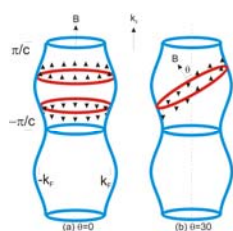


Fig. 3 – AMRO in a barrel shaped Fermi surface.

## Experimental

Single crystals of Tl2201 were fabricated using a self-flux method in alumina crucibles. As grown crystals are overdoped and their  $T_c$  was set by annealing in oxygen or argon. Electrical contacts were attached using Dupont 6838 silver paste. Inter-plane resistance measurements were carried out on a number of crystals (approx.  $300\mu m \times 150\mu m \times 20\mu m$ ) in the 45T hybrid magnet at NHMFL, Tallahassee, Florida using a two axis rotator probe. Data was taken over a large  $\theta$  range for five different  $\phi$  – typical data is shown in Fig. 4.

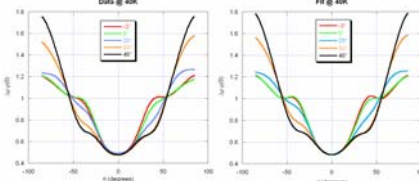


Fig. 4 – Left: Data at 40K ( $T_c=15K$ ). Right: Fit to same data.

## Analysis

We have shown previously that the Shockley-Chambers tube integral form of the Boltzmann transport equation can be used along with a 3D dispersion relation to accurately fit Tl2201 AMRO [4]. We expand  $k_F$  in cylindrical harmonics [6] where  $k = k_c c / 2$

$$k_F(\phi, \kappa) = \sum_{m=0}^{\infty} k_{mm} \begin{Bmatrix} \cos \\ \sin \end{Bmatrix} m\kappa \times \begin{Bmatrix} \cos \\ \sin \end{Bmatrix} m\phi$$

By considering the symmetry of the body-centered tetragonal lattice and that due to the role of the oxygen bonding orbitals in mediating it, the interplane hopping is dominated by hopping between adjacent planes, we expand to the lowest order necessary to fit the data.

$$k_F = k_{00} + k_{40} \cos 4\phi + k_{21} \cos \kappa (\sin 2\phi + \frac{k_{61}}{k_{21}} \sin 6\phi + \frac{k_{101}}{k_{21}} \sin 10\phi)$$

The Shockley-Chambers tube integral form of the Boltzmann transport equation can be expressed for a quasi-2D system in a periodic form,

$$\sigma_{zz} = \int_{-2\pi/c}^{2\pi/c} \cos \theta dk_z \int_0^{2\pi} d\phi \int_0^{\infty} d\phi' v_z(\phi) e^{-\phi} \frac{m_c(\phi)}{\omega_c(\phi)} v_z(\phi' - \phi) e^{\phi'}$$

where,

$$v_z(\phi) = \frac{\partial E}{\partial k_z} = \sin \kappa (\sin 2\phi + \frac{k_{61}}{k_{21}} \sin 6\phi + \frac{k_{101}}{k_{21}} \sin 10\phi) \quad h = \frac{1}{\omega_c(\tau - \tau')} \quad g = \frac{1}{\omega_c \tau}$$

Expressing the parts of  $\sigma_{zz}$  periodic in  $\phi$  and  $\phi'$  as Fourier sums and performing a Laplace transform means  $\sigma_{zz}$  can be readily calculated. This proves to be sufficient to fit the data at 4.2K [4].

## Anisotropic Scattering

However, as temperature increases the fits worsen. We find that to fit the data (see Fig. 4) we need to relax the constraint that  $\omega_c \tau$  remains isotropic in the plane. We introduce anisotropy in both the in-plane velocity  $v_F(\phi) = v_F^0(1 + \beta \cos 4\phi)$  and scattering rate  $1/\tau(\phi) = (1 + \alpha \cos 4\phi)/\tau^0$  [5] in the simplest form compatible with the crystal symmetry. This has the effect of introducing anisotropy in  $\omega_c$ ,  $g$  and  $h$ ,

$$\omega_c(\phi, \theta) = e\mu_0 H \cos \theta \frac{k_F(\phi) \cdot v_F(\phi)}{h k_c(\phi)^2} \quad g = g(\phi) = \int_{\tau'}^{\tau} \frac{1}{\omega_c(\phi)\tau(\phi)} d\phi' \quad h = h(\phi) = g(\phi - \phi')$$

As there is no experimental evidence to suggest significant changes in the Fermi surface topography with temperature we fix the Fermi surface parameters ( $k_{00}$   $k_{40}$ ,  $k_{61}$  and  $k_{101}$ ) and  $\beta$  to their 4.2K values and allow only  $\alpha$  and  $\omega_c \tau^0$  to vary with temperature. This  $\phi$  dependent scattering rate can be re-expressed as the sum of an isotropic component and anisotropic component with the same symmetry as the superconducting d-wave gap. See Fig. 5.

$$\frac{1}{\omega_c^0 \tau(\phi)} = \frac{(1 + \alpha \cos 4\phi)}{\omega_c^0 \tau^0} = \frac{(1 - \alpha)}{\omega_c^0 \tau^0} + \frac{2\alpha \cos^2 2\phi}{\omega_c^0 \tau^0}$$

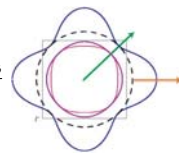


Fig. 5 – Right: Black dashed line – isotropic component of  $\tau$ . Blue line – anisotropic component of  $\tau$ . Red – 2D projection of the Fermi surface. Purple line – schematic representation of the d-wave superconducting gap.

## T Dependence of Anisotropic Scattering

We find that the isotropic component increases as  $T^2$  and the anisotropic component rises linearly with temperature from approximately zero at zero temperature, see Fig. 6.

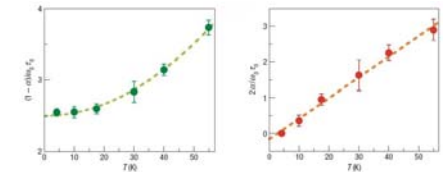


Fig. 6 – Left: Isotropic component of  $1/\tau(\phi)$  with  $A+BT^2$  fit. Right: anisotropic component of  $1/\tau(\phi)$  with  $C+DT$  fit.

## In-Plane Resistivity and Hall Coefficient

Using the anisotropic scattering parameters derived from our fits we can fit both the in-plane resistivity and the Hall coefficient at this doping using the Jones-Zener expansion of the linearised Boltzmann transport equation.

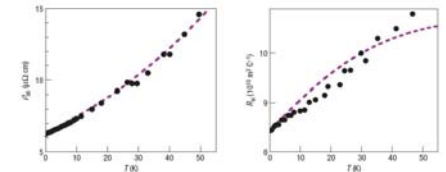


Fig. 7 – Left: In-plane resistivity. Right: Hall coefficient. Purple dashed line – fit, black dots – data extracted from [1]

Significantly, in non-superconducting cuprates, the in-plane resistivity varies as  $T^2$  at low temperatures with no evidence of a T-linear term [7]. This implies that the development of superconductivity (from the overdoped side) is closely correlated with the appearance of the T-linear resistivity and an anisotropic scattering rate.

## Doping Dependence of Anisotropic Scattering

From AMRO data taken at 40K on crystals with a range of  $T_c$  we find that the magnitude of this anisotropic component scales linearly with  $T_c$  [8]. Intriguingly this extrapolates to zero at the doping where superconductivity vanishes. The magnitude of the isotropic component remains constant with  $T_c$ .

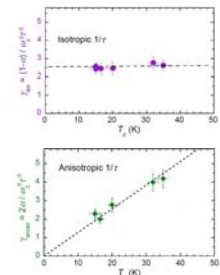


Fig. 8 – Top: Doping dependence of the isotropic component. Bottom: Doping dependence of the anisotropic component of  $1/\tau(\phi)$  at 40K.

## Conclusion

We have identified an anisotropic scattering rate in Tl2201 in which the isotropic component is proportional to  $T^2$  and is not dependent on doping. The anisotropic part is proportional to  $T$  and decreases linearly as doping is increased – disappearing at the doping level where superconductivity vanishes. The challenge now is to identify the origin of the anisotropic scattering and to confirm the linearity of the anisotropic scattering rate versus doping graph over a wider doping range.

## References

- [1] A. P. Mackenzie, PRB **53** 5848
- [2] M. Plate, PRL **95** 077001
- [3] K. Yamaji, JPSJ **58** 1520
- [4] N. Hussey, Nature **425** 814
- [5] M. Abdel-Jawad, Nature Physics **2** 821
- [6] C. Bergemann, Adv. Phys. **52** 639
- [7] S. Nakamae PRB **68** 100502
- [8] M. Abdel-Jawad, submitted to PRL